American Mineralogist, Volume 64, pages 687–700, 1979

Chain-width order and disorder in biopyriboles

DAVID R. VEBLEN AND PETER R. BUSECK

Departments of Geology and Chemistry, Arizona State University
Tempe, Arizona 85281

Abstract

High-resolution *c*-axis images of the biopyribole minerals anthophyllite [$(Mg,Fe)_7Si_8O_{22}(OH)_2$], jimthompsonite [$(Mg,Fe)_{10}Si_{12}O_{32}(OH)_4$], and chesterite [$(Mg,Fe)_{17}Si_{20}O_{54}(OH)_6$] have been produced in the transmission electron microscope. Interpretation of the images has been confirmed by dynamical electron diffraction and imaging calculations. In material from Chester, Vermont, the chain width of areas corresponding to more than one million amphibole chains in the *b* direction has been imaged and examined. In addition to perfectly ordered phases, parts of some crystals exhibit chain-width disorder ranging from minor faulting of otherwise ordered material to extreme disorder in the chain sequence. Individual silicate chains with widths corresponding to as many as 333 pyroxene chains have been observed. Several new ordered mixed-chain pyriboles have been found to occur in limited but statistically significant amounts. These new ordered structures have primitive unit-cell chain sequences (2233), (233), (232233), (222333), (2332323), (2333), (433323), (2234), and (43332343332423). A method for distinguishing statistically-significant ordered structures from those that arise simply from random combination of structural elements is described.

If the minerals chesterite and jimthompsonite are stable, their stability ranges are probably between those of anthophyllite and talc. The ordered minerals may, however, be produced metastably during reaction, as the result of constraints imposed by the reaction mechanisms. The occurrence of chesterite appears to be controlled by the chemical potentials of Fe, Ca, and Mg. The newly observed long-range ordered structures are probably the result of some non-random reaction or growth mechanism, rather than being thermodynamically stabilized.

Introduction

The common biopyribole minerals (micas, pyroxenes, and amphiboles) are of fundamental importance to the earth sciences. They play a key role in upper mantle petrology and are major components in many crustal rocks. They also figure heavily in some methods used to decipher the temperature and pressure histories of igneous and metamorphic rocks.

In addition to these common single-chain, double-chain, and sheet biopyriboles, other structurally ordered and closely related minerals have recently been found (Veblen and Burnham, 1975, 1976). These new biopyriboles contain triple silicate chains and alternating double and triple chains, and they belong to the biopyribole polysomatic series (Thompson, 1970, 1978). Their close structural relationships with the pyroxenes, amphiboles, and micas have been summarized by Veblen *et al.* (1977). Veblen and Burnham (1978a,b) have reported their detailed crystal structures, their chemical, physical, and optical properties, and their geological occurrence at Chester, Vermont.

The new biopyriboles were first recognized by single-crystal X-ray diffraction methods; refinements of X-ray data have provided a detailed structural understanding of the presently known groups of macroscopically ordered biopyriboles. However, it was recognized during the X-ray studies of material from Chester that many "single crystals" are really multiphase intergrowths, and streaking parallel to b^* on diffraction patterns further suggested that some pyribole[1] crystals are structurally disordered on a very fine scale in the *b* direction. We initiated the present high-resolution transmission electron microscopy (HRTEM) study in order to explore this disorder and its significance.

[1] "Pyriboles" are the biopyriboles excluding micas.

0003–004X/79/0708–0687$02.00

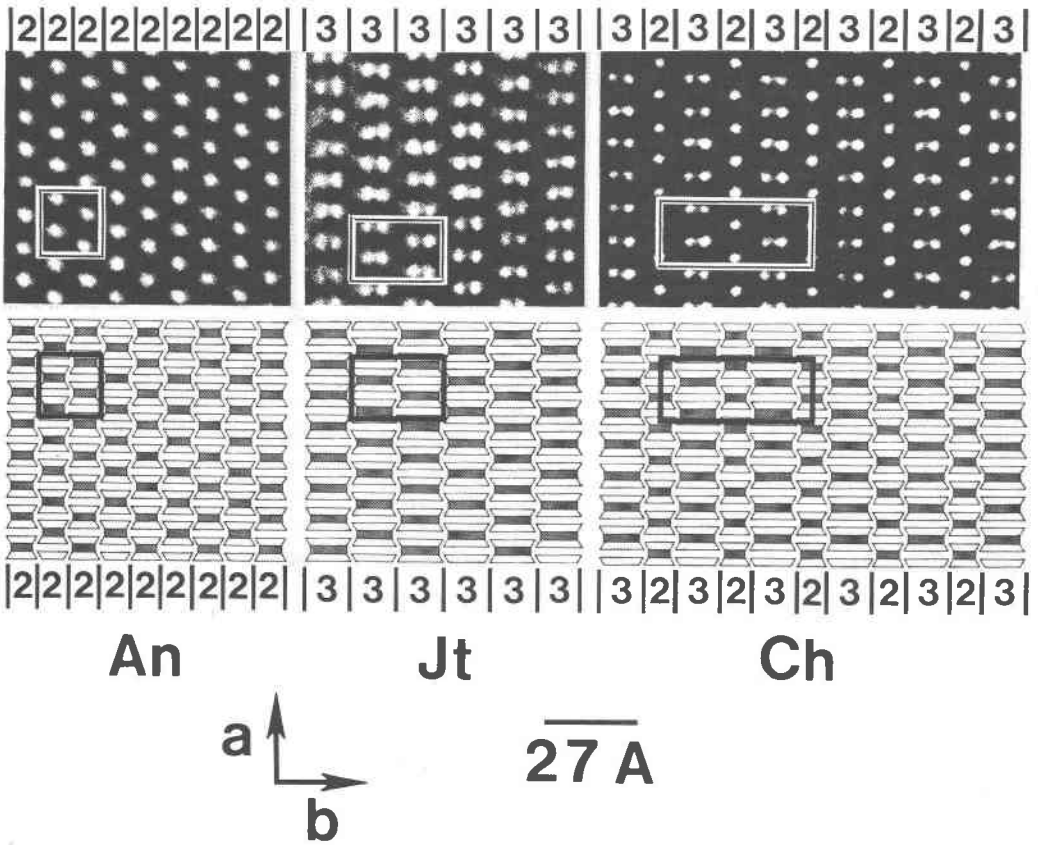

Fig. 1. HRTEM *c*-axis images of anthophyllite (An), jimthompsonite (Jt), and chesterite (Ch). The white spots are in the projected positions of the A-sites, which are located between the I-beams. Structural interpretation is shown in terms of I-beam diagrams, and unit cells and chain widths are indicated.

The feasibility of studying biopyriboles with HRTEM techniques was demonstrated by Buseck and Iijima (1974). Hutchison *et al.* (1975) showed that several fibrous amphiboles contain scattered units of triple-chain structure, confirming indications from an earlier, low-resolution study by Chisholm (1973). A study of nephrite actinolite (Hutchison *et al.*, 1976) revealed the presence of both triple- and sextuple-chain faults. The occurrence of chains of many different widths, up to the equivalent of 60 pyroxene chains, was reported by us in the material from Chester (Veblen *et al.*, 1977; Buseck and Veblen, 1978), as were several types of chain-terminating faults. Many of the same features were subsequently reported in nephrite (Jefferson *et al.*, 1978).

Most of the previous HRTEM studies of biopyriboles were done with the *a* or *b* axes parallel to the electron beam. In the present paper, we present new results obtained from electron diffraction and imaging experiments performed with the pyribole *c* axis parallel to the electron beam. This orientation permits unambiguous interpretation of the distribution of chains of various widths. We describe the HRTEM images produced by the ordered biopyriboles from Chester, as well as the nature of chain-width disorder found in these minerals. We also discuss the chemical nature of these structurally disordered regions and a number of new ordering schemes that have been found with HRTEM. In a subsequent paper we will present further results on the microstructures found in these minerals and their bearing on the behavior of biopyriboles during chemical reactions. In these studies, the chain width of areas corresponding to more than one million amphibole chains in the *b* direction has been imaged and examined.

The similarities among all the biopyribole groups that have been pointed out by Thompson (1970, 1978) emphasize that the relevance of the results presented here is not restricted to the unusual biopyriboles from Chester. Indeed, it has already been shown that analogous intergrowths occur in common pyroxenes, affecting their chemical and perhaps even

mechanical behavior (Smith, 1977; Veblen and Buseck, 1977; Buseck and Veblen, 1978; Yamaguchi *et al.*, 1978).

Experimental and sample preparation

Electron microscopy was performed with a JEM 100B microscope equipped with a modified top-entry goniometer stage, extra anti-contamination devices, and a nonconventional high-magnification intermediate lens. All photographs were obtained by imaging the beams passed by a 50 μm diameter objective aperture centered about the central beam. The microscope defocus values were between −700A and −1600A (see "Computed images" section), the condenser aperture diameter was 150 μm, and the accelerating potential was 100 kilovolts. Initial magnifications ranged from 200,000 to 500,000 times.

Specimens were prepared by three different methods. The *a*-axis images were obtained from specimens ground under acetone in an agate mortar and deposited on holey carbon grids. Some *c*-axis images were produced from specimens embedded in epoxy and then microtomed with a diamond knife. By far the largest number of images were obtained from epoxy-impregnated samples cut out of standard petrographic thin sections and then thinned by argon ion bombardment.

In the past, most HRTEM studies have employed crushed samples, and there has been concern that some observed defects may result from stresses arising during grinding. Because three different sample preparation techniques were employed in the present study, and similar results were obtained with samples prepared by each method, we conclude that the observed microstructures are not related to sample preparation. In particular, ion-thinned specimens are not subjected to great mechanical shear if care is taken in the preparation of the petrographic thin section from which the sample is removed, and the surfaces of the section that are damaged by grinding are removed during the thinning process. Direct correlation has been made between ordered and disordered regions of crystals identified optically in thin section and subsequently observed in the electron microscope, further suggesting that changes in chain width do not occur during ion milling.

One of the experimental difficulties encountered resulted from rapid electron beam damage of the specimen, as previously noted in anthophyllite by Hutchison *et al.* (1975). The rate of beam damage increased with chain width, and very wide chains, like talc, only survived for a few seconds in the beam before becoming amorphous and incapable of producing useable images. This difficulty was partially overcome by using ion-thinned specimens, which contained very large thin areas in approximately the same orientation. Images could be obtained by "sneaking up" on an undamaged area and photographing it immediately. Unfortunately, this approach also produces many poor images, since no time is allowed for cessation of stage drift.

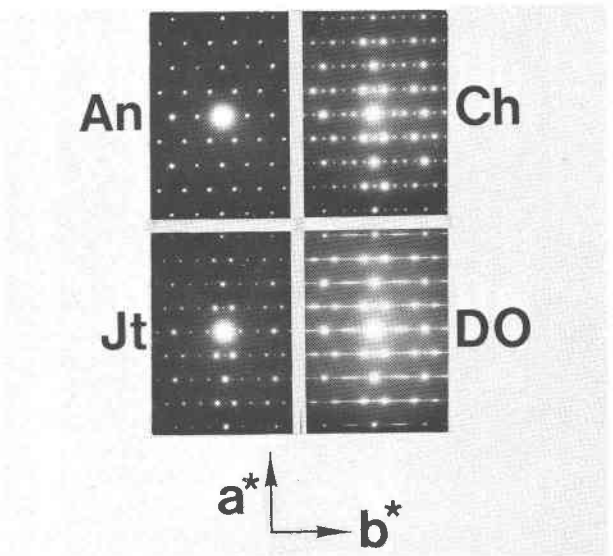

Fig. 2. *c*-axis electron diffraction patterns of anthophyllite, jimthompsonite, chesterite, and disordered chain silicate (DO) having a mixture of double, triple, and wider chains. The effects of different *b*-axis lengths can be seen in the ordered structures, while the disordered material produces streaks parallel to b^*.

Images of ordered biopyriboles

Intuitive interpretation

HRTEM images of biopyriboles can be interpreted by correlating the structures of ordered phases with the contrast they produce. Veblen *et al.* (1977) showed that biopyriboles of different groups, which can be recognized by their diagnostic diffraction patterns, produce distinctive images when viewed down their *a* axes. Similarly, *c*-axis images of ordered pyriboles (Fig. 1) can be correlated with their electron diffraction patterns (Fig. 2). Intepretation of the contrast in terms of pyribole I-beams is shown in Fig. 1 (see Veblen *et al.*, 1977, or Papike and Ross, 1970, for an explanation of I-beam diagrams).

"Intuitive" interpretation of this kind relies on the knowledge of structures derived by X-ray methods

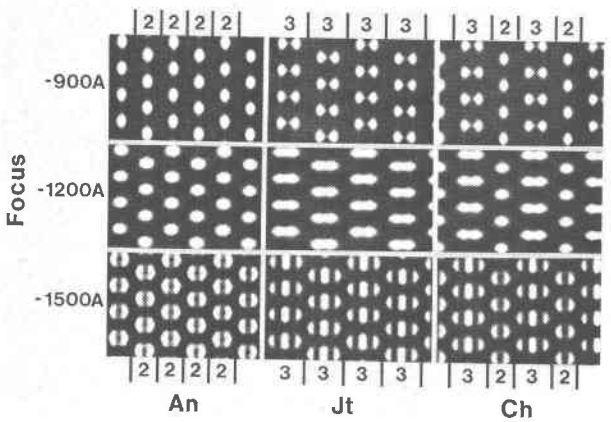

Fig. 3. Calculated *c*-axis HRTEM images of anthophyllite, jimthompsonite, and chesterite at three different values of defocus. Although there are changes in the detailed distribution of white spots with changes in focus, the positions of the I-beams are dark in all cases, and the widths of the silicate chains ("2" and "3") can be recognized. The images of Fig. 1 were taken near −900A defocus.

and on the somewhat fortuitous circumstance that, under appropriate experimental conditions, the image density may be closely related to the distribution of potential in the crystal (Cowley and Iijima, 1972). Thus, in the images in this paper, the positions of the I-beams appear dark, and triple-chain I-beams are easily differentiated by their widths from double-chain I-beams. Anthophyllite and jimthompsonite can be recognized by these *c*-axis structure images alone, and the rigorous alternation of double- and triple-chain I-beams in chesterite is evident (Fig. 1).

Computed images

Although a self-consistent picture is outlined above, a more rigorous confirmation of image interpretations can be derived from dynamical electron diffraction and imaging calculations, as outlined by O'Keefe *et al.* (1978). We have calculated *c*-axis images of anthophyllite, jimthompsonite, and chesterite using the SHRLI program package (M. A. O'Keefe, personal communication). Briefly, the computation process involves calculation of two-dimensional electron Fourier coefficients (structure factors) from refined atomic coordinates, temperature factors, and occupancies (Finger, 1970; Veblen and Burnham, 1978b). A total of 1513, 2315, and 5291 (*hk*0) Fourier coefficients were computed for anthophyllite, jimthompsonite, and chesterite, respectively. Fourier transformation of these coefficients then yields the projected potential in the crystal, as seen by the electron beam in the microscope. Dynamical diffraction amplitudes and phases are then calculated using the multislice formulation of Cowley and Moodie (1957), in which the crystal is represented as a series of discrete planes of projected potential at which diffraction takes place. A plane spacing (slice thickness) of 5.30A was used in our calculations; images from crystals of different thicknesses can be modeled by using different numbers of slices. The dynamical structure factors are then corrected for optical parameters and phase changes resulting from chromatic aberration, the size of the objective aperture, vibration, geometrical convergence of the primary electron beam, spherical aberration of the objective lens, and focus value of the microscope. A final Fourier transform of the resulting diffraction pattern yields the calculated image intensities, which are printed out in a halftone representation.

Some of the calculation results, for crystal thicknesses of 53A (10 unit cells), are shown in Figure 3. Although the detailed distribution of light and dark areas changes, recognizable and easily interpretable images occur over a large range of focus values (from about −700 to −1600A). It matters little that the images change somewhat with focus; in all cases the I-beam positions are shown by dark areas, and their widths are observable. Images with all the variations shown in Figure 3 have been observed experimentally for each of the ordered structures. The images of Figure 1 agree well with those calculated for −900A defocus, while some of the other image types can be seen in other figures of this paper and in papers now in preparation. Furthermore, multislice calculations have shown that the correspondence between dark areas on the images and I-beam positions is maintained up to a crystal thickness of about 250A.

Chains wider than triple

As indicated above, biopyribole chains wider than triple have been reported previously. However, most of these earlier observations were from *a*-axis images, and wide-chain structure is much easier to observe and interpret unambiguously in *c*-axis orientation. Figure 4 shows (010) slabs of quadruple- and quintuple-chain material in a matrix of disordered double- and triple-chain structure. Observations on ion-thinned specimens in this orientation confirm the observations of Veblen *et al.* (1977) that silicate chains of many different widths occur in the low-Ca chain silicates from Chester. It is difficult to record images of very wide chains, because the talc-like ma-

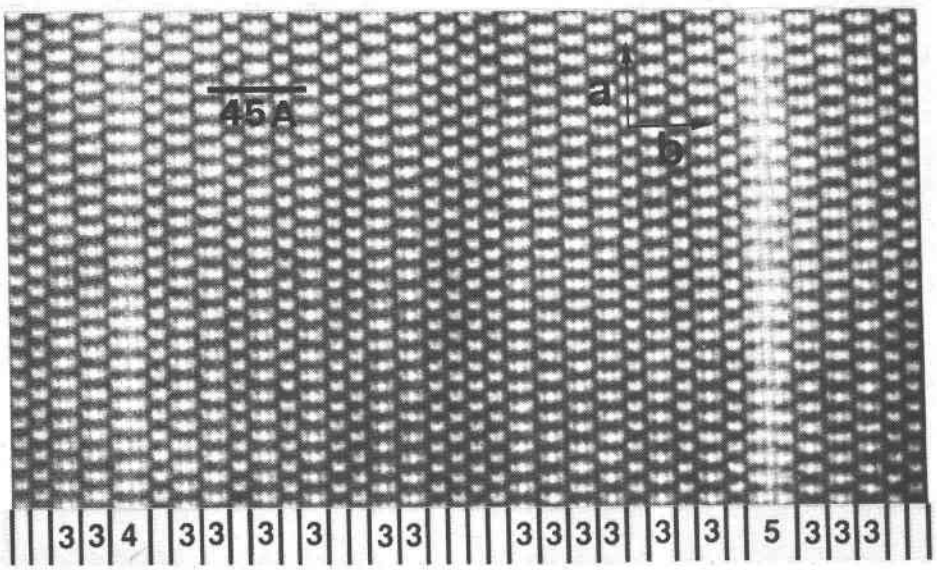

Fig. 4. An area containing double, triple, quadruple, and quintuple chains and exhibiting extreme chain-width disorder. Selected area diffraction patterns of material like this are similar to the disordered pattern of Fig. 2. Double-chain material is not labeled.

terial in the chain interiors suffers radiation damage and becomes amorphous after a few seconds in the electron beam. Neverthless, we have observed "chains" with widths equivalent to as many as 333 pyroxene chains (~1500A wide). Chains this wide might better be called "finite sheets," and they emphasize that there is a continuum of structures bridging the classical chain silicates (pyroxenes and amphiboles) and the sheet silicates.

Chemical composition of biopyribole with disordered chain widths

When examining electron micrographs of disordered chain silicates, it is often of interest to estimate the chemical compositions of certain regions. The structural formula of a region having a disordered sequence of chains can be determined by factoring the structure into mica (M) and pyroxene (P) slabs, as described by Thompson (1970, 1978). The number of M's in the region is multiplied by the talc formula $(Mg,Fe)_3Si_4O_{10}(OH)_2$, the number of P's is multiplied by the pyroxene formula $(Mg,Fe)_4Si_4O_{12}$, and the result is summed. Thus, for the chain sequence 2-2-2-4-3-6-3-2, we can factor to MP-MP-MP-MMMP-MMP-MMMMMP-MMP-MP, for a total of 16M's and 8P's. The composition is then $16(Mg,Fe)_3Si_4O_{10}(OH)_2 + 8(Mg,Fe)_4Si_4O_{12}$, which reduces to $(Mg,Fe)_{10}Si_{12}O_{32}(OH)_4$. The sequence in this example thus has a composition equivalent to that of jimthompsonite (MMP).

Microprobe analysis and occupancy refinement of the ordered minerals at Chester indicate that the outermost, distorted sites of the octahedral strips have an approximate composition of 0.2Mg + 0.8Fe in all the structures, while the more regular octahedral sites contain approximately 0.9Mg + 0.1Fe (Veblen and Burnham, 1978a,b). If these occupancies in the distorted and regular sites hold for disordered regions as well, an estimate of the Mg/Fe ratio could be derived by using the formula $Mg_{2.7}Fe_{0.3}Si_4O_{10}(OH)_2$ for the M slabs, and $Mg_{2.2}Fe_{1.8}Si_4O_{12}$ for the P slabs. It should be emphasized, of course, that compositions derived from structural formulae are not chemical analyses, but are based on assumptions of site occupancies.

Distribution of ordered and disordered material

In thin section, chesterite is commonly in contact with anthophyllite and jimthompsonite, but anthophyllite seldom touches jimthompsonite within a single grain (see Veblen and Burnham, 1978a, Fig. 2a–c; Veblen *et al., Science* cover, 28 October, 1977). This is a chemically logical arrangement of phases, because chesterite is compositionally intermediate between anthophyllite and jimthompsonite. Such a sequence is reminiscent of metasomatic zoning on a very fine scale. Structurally disordered material is found in all of the minerals, and, when viewed in thin section in the petrographic microscope, large portions of some grains show the (010) streaks characteristic of this disorder.

There is much less regularity in the spatial distribution of ordered and disordered material on the scale observable with HRTEM than on the macroscopic scale. Although it is common to find a zone of disordered pyribole at contacts between the ordered minerals, this is not always the case. Material that appears to be disordered in thin section may have any of several apparent types of structural disorder: (a) apparently random arrangements of double, triple, and wider chains; (b) bands of amphibole and triple-chain structure from several to dozens of chains wide, alternating with no intervening chesterite structure; or (c) any of the macroscopically-occurring ordered structures with numerous errors in chain width. In many cases, such disorder implies significant and irregular chemical fluctuations over short distances. It is not known what factors control the distribution of different disorder types. Major fluctuations in composition are, however, commonly observed in systems that are undergoing diffusion-controlled reactions (Prigogine, 1978; Nicolis and Prigogine, 1977).

New short-range pyriboles

Since the advent of HRTEM techniques, there have been several observations of ordered, short-range structural variations in synthetic and mineral systems. Such variations generally cannot be observed by X-ray methods. In the chain silicates from Chester, we have similarly recorded short-range ordered sequences. For discussions of these ordered pyriboles, it is convenient to denote their structures by the sequence of chains of different widths in a reduced unit cell. This repeating unit, which we enclose in parentheses, defines the ordered structure. Anthophyllite would thus be denoted as (2), jimthompsonite as (3), and chesterite as (23). In addition to these macroscopically occurring structures,[2] we have, for example, recorded as many as 15 repeats of the sequence (2233), and as many as 45 unfaulted repeats of (2333), as shown in Figure 5. These sequences produce reasonably sharp diffractions characteristic of 45A and 49½A *b* axes.

[2] By macroscopic structures we mean those that occur in crystals large enough to see with the naked eye. Although jimthompsonite and chesterite cannot be differentiated from anthophyllite in hand specimen, their crystal size in some cases exceeds ½mm × ½mm × several mm, and single crystals separated for X-ray analysis, for example, are clearly visible with the unaided eye. We therefore refer to anthophyllite, jimthompsonite, and chesterite as macroscopic phases.

In studying short-range sequences, it is necessary to have some means of distinguishing sequences of significance (those that arise for thermodynamic reasons or are the result of some growth or reaction mechanism) from those that occur simply from random combinations of structural elements. For example, Buseck and Iijima (1975) required a minimum of three repeats of a stacking sequence to qualify the sequence as a new structure type or polytype. Van Landuyt and Amelinckx (1975) required ten repeats in three different crystal fragments as a minimum before a structure could qualify as a new compound. Both these definitions, though simple to apply, are purely arbitrary. We will therefore now propose a statistical method that places the decision of significance on a more objective basis.

Probability calculation

If one were to search an infinite random sequence of double and triple chains, any ordered sequence could be found eventually. This is not done in practice, and it is therefore possible to use one-sample tests, such as a runs test, to check for randomness of any part of a sequence (Bradley, 1968, Ch. 11). A runs test examines the number of runs of different objects and compares it with the total numbers of the objects. (A run is a succession of one or more identical objects. The sequence AAABBB thus contains two runs, while ABABAB contains six.) If the number of runs is too great or too small, *i.e.*, if the number falls too far out on the tails of the probability distribution of the number of runs, then the sequence is declared non-random (Swed and Eisenhart, 1943). Thus, events with low probabilities of occurring randomly are singled out as being significant.

Similarly, we can calculate the probability that an ordered sequence will occur in a crystal as a result of random placement of structural elements. We may then choose a threshold probability, say 0.001, and accept a sequence as significant if its probability of occurring randomly is less than this value. Given that the first repeat unit of an ordered sequence has occurred, we want to know the probability that it will be repeated as observed through a purely random process. In a crystal consisting of A's and B's, to calculate this probability we disregard the first unit and assume that we are sampling a population having the same number of A's and B's as the remaining part of the sequence. If the number of A's is n_A and the number of B's is n_B, then the probability of randomly sampling an A is simply $n_A/(n_A + n_B)$. The com-

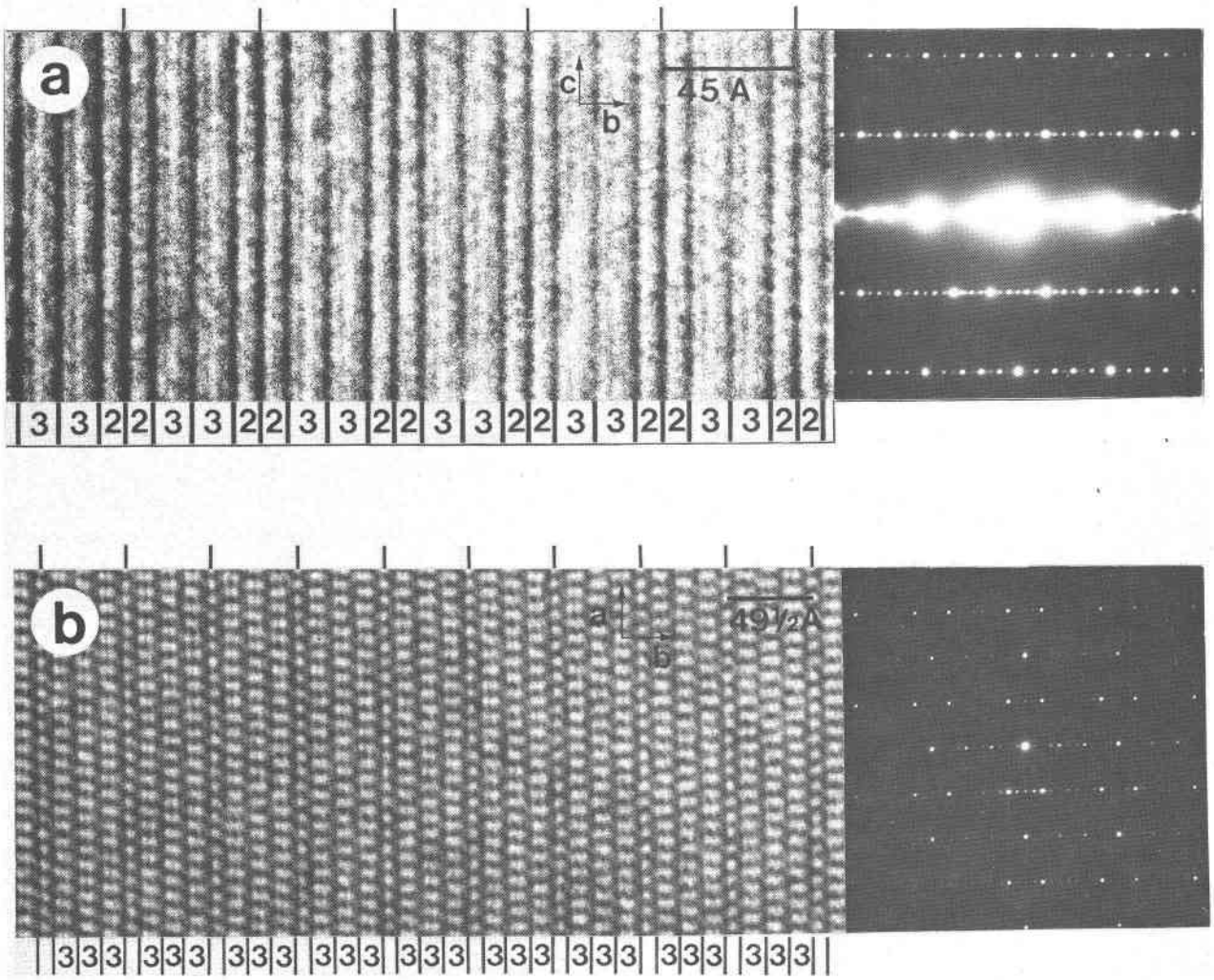

Fig. 5. (a) An *a*-axis image of chain silicate with the ordering scheme (2233). The diffraction pattern has a periodicity characteristic of $b = 45$A, which is twice the periodicity shown by *a*-axis patterns of chesterite (see Veblen *et al.*, 1977). Unit-cell spacing is indicated by marks above image. (b) A *c*-axis image of chain silicate with the ordering scheme (2333). The double-chain slabs are unlabeled. The diffraction pattern has a periodicity characteristic of $b = 49½$A.

pound probability of randomly obtaining the sequence in question is then

$$p = (n_A!n_B!)/(n_A + n_B)!$$

where n_A and n_B represent the number of A's and B's in the sequence, after removing the first unit. For structures containing more than two types of structural elements, this can be generalized to

$$p = \frac{n_1!n_2!n_3! \cdots}{(n_1 + n_2 + n_3 \cdots)!}$$

This probability expression could, for example, be applied to sequences of stacking operators in mica polytypes or other polytypic materials.

It must be emphasized that the choice of structure elements (A's and B's) is critical for an analysis of this sort. The elements chosen must behave independently in the structures being analyzed. Because double, triple, and quadruple chains occur as isolated structural elements in disordered regions, they may be considered to act independently in the Chester pyriboles. The choice of M and P slabs as the structural elements would be inappropriate, for example, because a P slab is always followed by an M slab in the Chester occurrence. Furthermore, although the use of M's and P's might tell us whether or not M and P slabs combine in a nonrandom fashion, in the Chester pyriboles we are instead interested in know-

Table 1. Chain sequences of observed ordered pyriboles

Sequence	Observed Repeats	Probability p	Site Composition	Repeat Length (A)**	Maximum Symmetry***	Comments
(2)	--*	--*	MP	9	Pnma	Anthophyllite
(3)	--*	--*	M_2P	13½	Pbca	Jimthompsonite
(23)	--*	--*	M_3P_2	22½	$A2_1ma$	Chesterite
(2233)	15	1.31×10^{-16}	M_3P_2	45	$P2_1/a$	Fig. 5a
(233)	11	3.33×10^{-8}	M_5P_3	36	Pnma	
(232233)	4	2.06×10^{-5}	M_3P_2	67½	Pa	
(222333)	3	1.08×10^{-3}	M_3P_2	67½	$A2_1ma$	
(2332323)	3	3.33×10^{-4}	$M_{11}P_7$	81	$P2_1/a$	
†(2333)	45	1.62×10^{-42}	M_7P_4	49½	$A2_1ma$	Figs. 5b and 7
†(433323)	5	1.94×10^{-8}	M_2P	81	Pa	Fig. 7
†(43332343332423)	4	5.82×10^{-17}	M_2P	189	Pa	Fig. 7
†(2234)	4	5.41×10^{-5}	M_7P_4	49½	Pa	Fig. 7

* Longest observed runs of unfaulted material are macroscopic.

** Length of one repeat of the sequence in the b* direction.

*** Retaining the usual amphibole-pyroxene axes, with c as the chain direction and a as the stacking direction. Assumes ++-- stacking.

† Taken from the sequence diagrammed in Fig. 6.

ing whether double, triple, and quadruple chains combine nonrandomly.

Observed pyribole polysomes

Ordered sequences of double, triple, and quadruple chains observed in the Chester pyriboles are tabulated in Table 1. The repeated unit is given in the first column, followed by the maximum number of times it has been seen to repeat, the probability p, as defined above, the structural formula given in terms of M $[(Mg,Fe)_3Si_4O_{10}(OH)_2]$ and P $[(Mg,Fe)_4Si_4O_{12}]$ units, the length of the repeating unit in the b^* direction, and the maximum space-group symmetry for the material, assuming the typical orthopyribole ++−− stacking sequence. With the exception of (222333), polysomes with p values greater than 0.001 have been excluded from Table 1.

The low values of p (as low as 1.62×10^{-42} for the newly-observed polysomes) suggest that most, if not all, of the structures given in Table 1 are statistically significant. This means that they have arisen either as the result of their thermodynamic properties or as the result of some directed crystal growth or reaction process, rather than from a purely random process.

Non-random disorder

An observation that may be related to the occurrence of rare polysomes concerns the nature of chain-width errors in chesterite. When the rigorous alternation of double and triple chains in this mineral is interrupted by an extra double chain, for example, the error is frequently compensated by an extra triple chain. Thus, an isolated unit of (2233) occurs in chesterite more frequently than uncompensated extra double chains or extra triple chains. In places, the compensation does not occur immediately, but leads to an isolated error of the sort (223233) embedded in otherwise normal chesterite. The same sort of compensation is observed where more than one extra chain of a given width is inserted, leading to isolated faults such as (222333) and (22223333). Faults of the types (2233), (222333), and (332322) are shown in Figure 6.

Although uncompensated extra chains do occur as

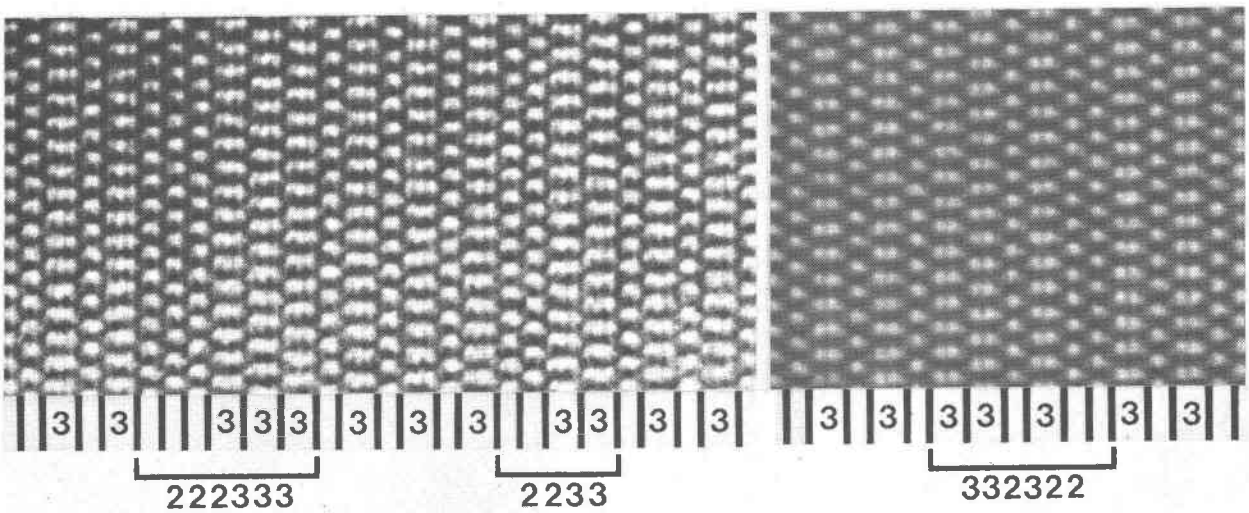

Fig. 6. Faults in chesterite of the type (2233), (222333), and (332322). Chain-width errors in chesterite are commonly of these types, in which an excess of double chains is locally compensated by an equal excess of triple chains.

faults in chesterite, the greater frequency of compensated faults suggests that for some reason they are more favorable. The uncompensated chain-width errors imply a change in stoichiometry, while the compensated faults maintain the chesterite site composition. The fact that the chain sequences in the compensated faults are also observed as ordered polysomes [see (2233) and (222333) in Table 1] suggests that the isolated faults and some of these polysomes may have related origins.

Formation of short-range polysomes

Several features of the polysomes listed in Table 1 may bear on their mode of formation. First, there are compositional coincidences in the site formulas, notably at M_2P, M_3P_2, and M_7P_4, of which the first two correspond to the jimthompsonite and chesterite compositions. These coincidences suggest from phase-rule considerations that most of the short-range polysomes are, at best, metastable. Although chemical analyses are not available, the notion that these short-range polysomes are stabilized by chemical elements not observed in the macroscopic pyriboles is unlikely, considering the chemical and structural regularity exhibited by the anthophyllite, chesterite, and jimthompsonite. The extreme complexity of some of the short-range polysomes, such as the polymorph of jimthompsonite (43332343332423), further suggests that they arose not because they have lower free energies than other arrangements of chains, but rather as the result of some growth or reaction mechanism.

Spiral growth about a screw dislocation can produce a variety of polytypes in numerous substances (Verma and Krishna, 1966; Trigunayat and Verma, 1976), and if layers of different compositions and structures are involved, such a growth mechanism could also create a variety of polysomes. It is also possible to grow a crystal by a screw-dislocation mechanism and subsequently transform it to other polytypes by a reaction that travels around the original growth spiral (Kiflawi *et al.*, 1976).

Abundant textural and microstructural evidence suggests that the pyriboles at Chester with chains wider than double arose by solid-state reaction from anthophyllite and not from a primary growth process (Veblen and Burnham, 1978a; Veblen *et al.*, 1977; Veblen and Buseck, in preparation). This does not, however, completely preclude a screw-dislocation growth mechanism for the observed but rare short-range polysomes. Small parts of some mixed-chain crystals could have grown in fractures opened up during deformation and retrograde metamorphism.

Certain aspects of the distribution of short-range pyriboles are not readily explicable by a screw-dislocation model. The last four polysomes listed in Table 1 were all observed intergrown with areas of jimthompsonite and chesterite structure in a small region (~1.5 μm wide) of an otherwise well-ordered anthophyllite crystal. Their spatial distribution in this region is schematically shown in Figure 7; domains of various polysomes are labeled by the chain sequence in the repeating unit, while domains of disordered material are labeled "DO." There are several

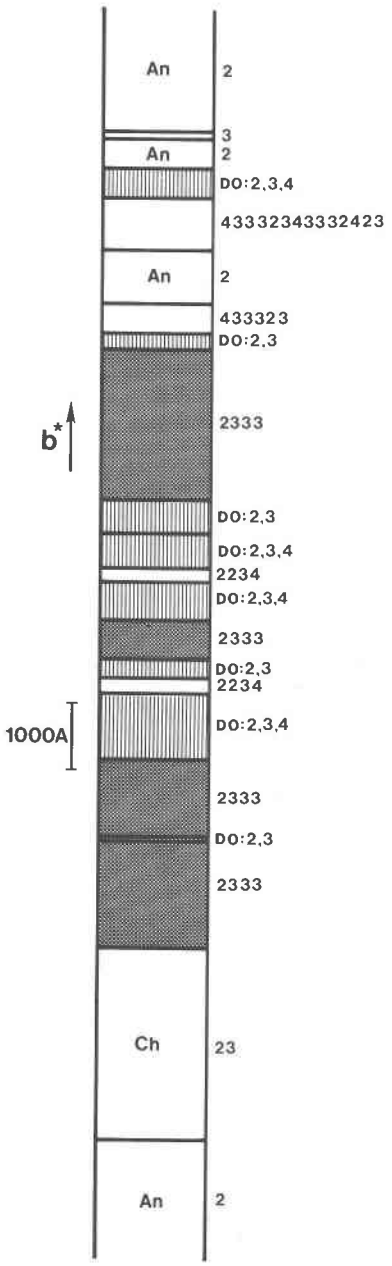

Fig. 7. A diagram of part of a crystal containing short-range ordered polysomes. The ordering schemes of the various domains are indicated by the primitive unit-cell chain sequences. Disordered material containing only double and triple chains is denoted by "DO-2,3," while that which also contains quadruple chains is labeled "DO-2,3,4." The polysome (2333) is shaded to emphasize that it occurs in not one, but several domains, separated by both disordered and ordered material. Lighter shading indicates disordered chain silicate.

distinct areas of (2333) structure separated by disordered material containing double, triple, and quadruple chains, and in two of these disordered areas there are short ordered sequences of (2234). If the (2333) structure grew fortuitously by a screw-dislocation mechanism, there is no obvious reason why the structure would reappear after being interrupted by the growth of disordered material; this is the only area in which (2333) has been observed. Likewise, if all the areas of (2333) grew by spiral growth as a single domain which was subsequently altered by reaction to disordered material, there is no ready explanation for the occurrence of ordered (2234) structure between (2333) domains.

Although (2333) and (2234) have the same repeat length in the b^* direction (49½A), (433323) and (43332343332423) have different lengths and would therefore require growth ledges of different heights; this would complicate a screw-dislocation model for their production. Another puzzling observation, although perhaps coincidental, is that (433323) is included as a part of the sequence (43332343332423), and (2333) is part of both of them.

To summarize, neither the ordered polysomes in Figure 7 nor the isolated compensated faults in chesterite are explained satisfactorily by a screw-dislocation growth model. A model involving reaction of amphibole that initially grew by a spiral growth mechanism is subject to some of the same problems, although it is more consistent with textural observations suggesting that the wide-chain pyriboles arose by reaction from amphibole. We thus have no satisfactory explanation for the existence and mode of occurrence of these rare polysomes. A suitable explanation might, however, yield a good deal of information about the behavior of biopyriboles during growth and reaction.

Stabilities of Mg,Fe biopyriboles

In the absence of petrologic experiments, it is not possible to state whether or not jimthompsonite, chesterite, and their monoclinic polymorphs are stable phases. Indeed, the structural disorder of the amphibole grown in anthophyllite stability studies (Veblen and Buseck, in preparation) indicates that such experiments would be exceedingly difficult. By considering the Mg,Fe biopyribole occurrence at Chester, Vermont, we can, however, obtain some useful insights into this problem.

Hypothetical free-energy diagram

Because chesterite and jimthompsonite (and their monoclinic analogs) occur macroscopically in well-ordered states, it is clear that under some conditions they must be more stable than a random disordered array of double, triple, quadruple, and wider chains

having the same bulk composition. Similarly, we know from the widespread occurrence of amphiboles that pure double-chain pyriboles are stable relative to a hypothetical pyribole of the same composition with, for example, single and quadruple chains in a 2:1 ratio. In fact, for any pyribole composition between enstatite and talc, there is presumably a pyribole structure that has the optimum chain sequence and lowest possible free energy for a given set of physical conditions. Likewise, every composition will have a "worst case" structure that has a maximum free energy. Based on these considerations, we can hypothesize a free energy *vs.* composition diagram, such as the one in Figure 8, in which any given composition has a range of possible free energies based on its structural state. In terms of ratios of chains with different widths, only the end-members, enstatite and talc, have uniquely determined structures, neglecting polytypic variations (any intermediate composition could be constructed as a mixture of chains of various widths). Therefore, only enstatite and talc are shown as having unique free energies in Figure 8.

Figure 8 is, of course, only a cartoon of the real situation. Because enstatite and anthophyllite represent energy minima, a "structure" containing extremely wide slabs of enstatite and anthophyllite (or a rock containing separate enstatite and anthophyllite grains) would have a free energy that is nearly a linear combination of these two minima. In the present case of homogeneous replacement of one biopyribole by another, we can ignore such structures composed of very wide slabs, however, because they apparently are precluded by the mechanisms of reaction. Figure 8 is thus specific for situations similar to that observed at Chester, where the reaction mechanisms constrain the range of possible structures to the shaded area.

Because chesterite and jimthompsonite represent a sizable volume of the Chester pyribole material, compared with disordered intermediate compositions, these ordered minerals presumably represent local free-energy minima, as shown in Figure 8. Although chesterite and jimthompsonite may well be stable under some conditions, the diagram has been drawn showing them metastable with respect to anthophyllite plus talc. If this is the actual case, then chesterite and jimthompsonite are intermediate metastable phases occurring during a reaction, and they might well be thought of as Ostwald steps (Ostwald, 1897; Verma and Krishna, 1966, p. 21). Another minimum in Figure 8 has been placed at the PMP composition, where a hypothetical pyribole with alternating single and double chains might be found to occur during enstatite–anthophyllite reactions. The occurrence of this silicate between enstatite and anthophyllite would be analogous to that of chesterite between anthophyllite and jimthompsonite (Veblen and Burnham, 1976; Veblen *et al.*, 1977). In addition to the free-energy minima shown in Figure 8, there are probably other small wiggles in the lower line corresponding to compositions at which favorable structures are possible. The structure (2333), for example, could represent a minimum, but the observed short-range pyriboles have been ignored in Figure 8 because they presumably form as a result of growth or reaction mechanisms.

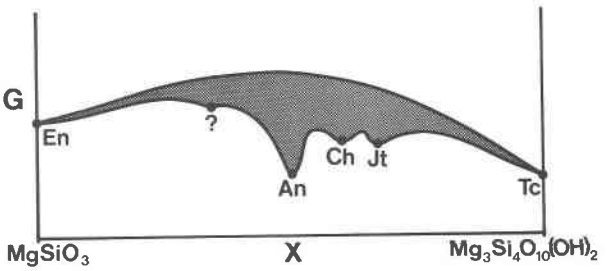

Fig. 8. A hypothetical free energy (G) *vs.* composition (X) diagram at arbitrary temperature and pressure. For any given composition, there is a range of possible free energies corresponding to different sequences of single, double, triple, and wider chains. Chesterite and jimthompsonite are shown here as metastable energy minima between anthophyllite and talc, and another minimum labeled "?" has been placed at the composition of a hypothetical structure with rigorously alternating single and double chains.

Hypothetical phase diagrams

If chesterite and jimthompsonite are metastable for all pressures and temperatures, then they will not, of course, appear on an equilibrium phase diagram. If they are stable, then their structural, chemical, and textural relations strongly suggest that they will occur between the anthophyllite and talc stability ranges. This can be shown on an isobaric temperature *vs.* activity of SiO_2 diagram, such as employed by Hemley *et al.* (1977). Figure 9 shows such a diagram with narrow stability fields for chesterite and jimthompsonite inserted between anthophyllite and enstatite. The location of these possible stability ranges is analogous to the field of formation of pyribole asbestos suggested by Ross (1978).

An interesting problem in biopyribole stabilities is presented by a thin section from a different part of the Chester blackwall zone from that utilized in this study. In this thin section, which was kindly supplied

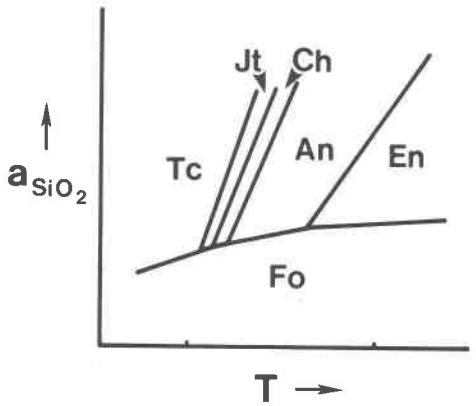

Fig. 9. A hypothetical activity of SiO_2 *vs.* temperature diagram showing the probable locations of the chesterite and jimthompsonite stability fields with respect to those of talc, anthophyllite, enstatite, and forsterite. The diagram assumes that chesterite and jimthompsonite are stable.

by John Rosenfeld, the mineral chesterite is absent at the resolution of the light microscope. Anthophyllite and jimthompsonite coexist with sharp contacts, and there is also some disordered material present (Fig. 10). Since the pressure–temperature regime during metamorphism probably did not differ significantly in different parts of the small ultramafic body at Chester, a difference in some other parameter, such as the chemical potential of some component, must account for the absence of chesterite in this speci-

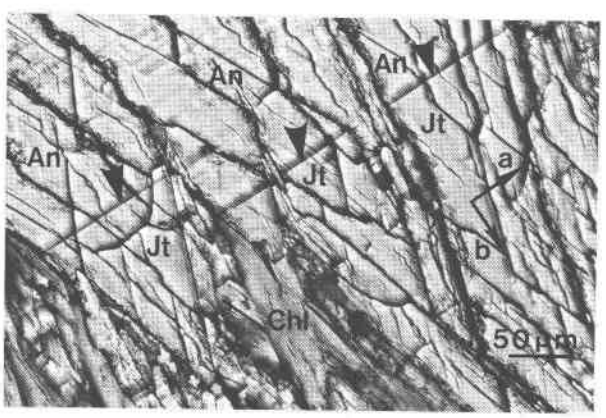

Fig. 10. A petrographic thin section from assemblage #2, Chester, Vermont (see Table 2). Anthophyllite and jimthompsonite meet at sharp contacts, and chesterite is entirely absent, suggesting that the stable or metastable occurrence of chesterite is controlled by some factor other than temperature or pressure. Streaking parallel to (010) in anthophyllite results from minor structural disorder, and chlorite (Chl) is also present. The lower cleavage angle of jimthompsonite (37°) compared to that of anthophyllite (54°) can be seen by sighting along the cleavage planes at a low angle and noting the change in direction when the fractures cross the phase boundary. Crossed polars.

Table 2. Microprobe analyses of anthophyllite (Anth) and jimthompsonite (Jt) in two different specimens from Chester, Vermont

	Anth #2†	Anth #1	Jt #2	Jt #1
SiO_2	56.6	56.2	58.3	57.2
Al_2O_3	0.7	0.7	0.9	0.9
MgO	24.0	23.0	25.7	24.4
FeO*	14.4	15.8	11.1	12.6
CaO	1.2	0.5	0.7	0.4
MnO	1.2	1.1	0.7	0.8
Na_2O	0.2	0.1	0.3	0.2
H_2O**	2.1	2.1	2.9	2.9
Total	100.4	99.5	100.6	99.4
	Structural Formulae			
Number of oxygens	23	23	34	34
Tetrahedral:				
Si	7.90	7.94	11.85	11.85
Al	0.10	0.06	0.15	0.15
Total	8.00	8.00	12.00	12.00
Octahedral:				
Al	0.02	0.05	0.05	0.07
Mg	4.98	4.86	7.78	7.52
Fe*	1.68	1.87	1.88	2.18
Ca	0.18	0.08	0.15	0.08
Mn	0.15	0.13	0.13	0.13
Total	7.01	6.99	9.99	9.98
A-site:				
Na	0.03	0.02	0.06	0.05
$Na+Al^{VI}-Al^{IV}$	-0.05	+0.01	-0.04	-0.03
H_2O**	1.00	1.00	2.00	2.00

†Anth #1 *and* Jt #1: *Veblen and Burnham (1978a);* Anth #2 *and* Jt #2: *material supplied by J. Rosenfeld from same talc quarry at Chester, Vermont.*
**All iron calculated as* Fe^{2+}.
***The amount of water was calculated by assuming all OH sites to be filled with* OH^- *(Veblen and Burnham, 1978a, b).*

men. Chemical analyses (Table 2)[3] show that anthophyllite #2 and jimthompsonite #2 contain twice as much calcium, more magnesium, and less iron than the material described by Veblen and Burnham (1978a), while the concentrations of other species are roughly the same for the two samples. This relationship strongly suggests that the chesterite structure is destabilized either by increasing the Ca/Fe ratio in

[3] Energy-dispersive analyses were performed on flat polished specimens with a JEOL JXA35 analytical SEM and a PGT1000 spectrometer. The spectra were fit by least squares, following a hyperbolic background subtraction based on theoretical bremsstrahlung calculations. Standard FRAME correction procedures were used, and the analyses were renormalized using an amphibole standard.

the outermost, distorted octahedral sites or by increasing the Mg/Fe ratio in the regular octahedral sites. The chemical potentials of Ca, Fe, and Mg thus appear to control chesterite stability. The observed chemical variations could be the result of a reduced chemical potential of Fe in assemblage #2; Figure 11 is a temperature *vs.* activity of FeO diagram consistent with this possibility. Although there is no compelling structural reason that octahedral cation ratios should control the presence of chesterite, the same phenomenon appears to be true for anthophyllite, which is stabilized by higher Fe/Mg ratios relative to talc plus enstatite (Evans and Trommsdorff, 1974).

Although the question of stability *vs.* metastability for the ordered triple- and mixed-chain silicates at Chester is unresolved, there are other chemical systems in which these stability fields may be much larger and more easily tested. For example, triple-chain silicate rather than amphibole may well be the stable phase around 500 to 600°C in systems containing both Na and Mg (Drits *et al.*, 1974, 1976; Tateyama *et al.*, 1978). In light of the experiments by Drits *et al.* and the difficulties involved in anthophyllite stability studies, it would be premature to reject out of hand the possibility that jimthompsonite and chesterite are stable phases in the MgFe biopyribole system.

Conclusions

1. The feasibility and value of studying structurally complex biopyriboles with high-resolution transmission electron microscopy have been established.

2. Silicate "chains" with widths equivalent to as many as 333 pyroxene chains have been observed in biopyribole from Chester, Vermont. The distinction between material with chains this wide and talc is probably mainly semantic.

3. Compositions of biopyribole with disordered chain sequences can be approximated by factoring the structure into M (mica) and P (pyroxene) modules, after Thompson (1978).

4. On the scale visible with the petrographic microscope, the chain silicates from Chester are distributed in a chemically and structurally logical fashion, with chesterite generally occurring between anthophyllite and jimthompsonite. On the scale observable with HRTEM, there is much less regularity in the distribution of phases in fairly disordered regions and in the nature of extremely disordered regions.

5. Several new short-range ordered pyriboles have been observed. The probability that they all arose from random grouping of chains of various widths is miniscule. The mechanism for generating these rare polysomes is unknown.

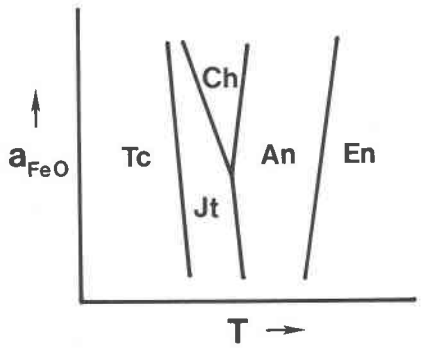

Fig. 11. A hypothetical activity of FeO *vs.* temperature diagram that assumes chesterite and jimthompsonite to be stable. The diagram is consistent with the observation that chesterite is absent in assemblage #2, which has lower Fe/Ca and Fe/Mg ratios than corresponding phases of assemblage #1 (Table 2).

6. It is not known whether chesterite and jimthompsonite have fields of stability or were produced metastably. If stable, their stability fields probably lie between those of anthophyllite and talc. During hydration reactions, a pyribole crystal may be constrained by the reaction mechanisms to follow a thermodynamic potential path on which jimthompsonite and chesterite represent free-energy minima. The occurrence of chesterite is apparently determined by the chemical potentials of Ca, Fe, and Mg.

Acknowledgments

We thank Dr. Michael A. O'Keefe for helping us perform dynamical imaging calculations and Mr. Gary D. Aden and Dr. John T. Armstrong for help with the microprobe analyses. Dr. Dennis L. Young of the Arizona State University Department of Mathematics provided helpful discussions on one-sample statistical tests. Dr. John L. Rosenfeld kindly supplied an important specimen that he collected from the Chester quarry. Helpful reviews were provided by Drs. Charles W. Burnham, Cornelis Klein, Ian D. R. Mackinnon, and Paul H. Ribbe. Electron microscopy was performed in the Electron Microscope Facility of the Center for Solid State Science, and the chemical analyses were obtained in the Electron Microprobe Laboratory of the Department of Chemistry, Arizona State University. Financial support was provided by NSF grant EAR 77-00128 (Earth Sciences).

References

Bradley, J. V. (1968) *Distribution-free Statistical Tests.* Prentice-Hall, Englewood Cliffs, New Jersey.

Buseck, P. R. and S. Iijima (1974) High resolution electron microscopy of silicates. *Am. Mineral., 59,* 1–21.

——— and ——— (1975) High resolution electron microscopy of enstatite II: geological application. *Am. Mineral., 60,* 771–784.

——— and D. R. Veblen (1978) Trace elements, crystal defects

and high resolution electron microscopy. *Geochim. Cosmochim. Acta, 42,* 669–678.

Chisholm, J. E. (1973) Planar defects in fibrous amphiboles. *J. Mater. Sci., 8,* 475–483.

Cowley, J. M. and S. Iijima (1972) Electron microscope image contrast for thin crystals. *Z. Naturforsch., 27a,* 445–451.

——— and A. F. Moodie (1957) The scattering of electrons by atoms and crystals. I. A new theoretical approach. *Acta Crystallogr., 10,* 609–619.

Drits, V. A., Y. I. Goncharov, V. A. Aleksandrova, V. E. Khadzhi and A. L. Dmitrik (1974) New type of strip silicate. *Kristallografiya, 19,* 1186–1193 (transl. *Sov. Phys. Crystallogr., 19,* 737–741).

———, ——— and I. P. Khadzhi (1976) Formation conditions and physico-chemical constitution of triple chain silicate with $[Si_6O_{16}]$ radical. (in Russian) *Izv. Akad. Nauk., Ser. Geol., 7,* 32–41.

Evans, B. W. and V. Trommsdorff (1974) Stability of enstatite + talc, and CO_2-metasomatism of metaperidotite, Val d'Efra, Lepontine Alps. *Am. J. Sci., 274,* 274–296.

Finger, L. W. (1970) Refinement of the crystal structure of an anthophyllite. *Carnegie Inst. Wash. Year Book, 68,* 283–288.

Hemley, J. J., J. W. Montoya, D. R. Shaw and R. W. Luce (1977) Mineral equilibria in the MgO–SiO_2–H_2O system: II. Talc–antigorite–forsterite–anthophyllite–enstatite stability relations and some geologic implications in the system. *Am. J. Sci., 277,* 353–383.

Hutchison, J. L., M. C. Irusteta and E. J. W. Whittaker (1975) High resolution electron microscopy and diffraction studies of fibrous amphiboles. *Acta Crystallogr., A31,* 794–801.

———, D. A. Jefferson, L. G. Mallinson and J. M. Thomas (1976) Structural irregularities in nephrite jade: an electron microscope study. *Mater. Res. Bull., 11,* 1557–1562.

Jefferson, D. A., L. G. Mallinson, J. L. Hutchison and J. M. Thomas (1978) Multiple-chain and other unusual faults in amphiboles. *Contrib. Mineral. Petrol., 66,* 1–4.

Kiflawi, I., Z. H. Kalman and Y. Sonnenblick (1976) Direct observation of polytype transformations in a vapour-phase grown ZnS crystal. *J. Cryst. Growth, 34,* 145–148.

Nicolis, G. and I. Prigogine (1977) *Self-organization in Nonequilibrium Systems.* Wiley-Interscience, New York.

O'Keefe, M.A., P. R. Buseck and S. Iijima (1978) Computed crystal structure images for high resolution electron microscopy. *Nature, 274,* 322–324.

Ostwald, W. (1897) The formation and changes of solids. (in German) *Z. Phys. Chem., 22,* 289–330.

Papike, J. J. and M. Ross (1970) Gedrites: crystal structures and intracrystalline cation distributions. *Am. Mineral., 55,* 1945–1972.

Prigogine, I. (1978) Time, structure, and fluctuations. *Science, 201,* 771–785.

Ross, M. (1978) The "asbestos" minerals: definitions, descriptions, and health effects. In C. C. Gravatt, Ed., *Workshop on Asbestos: Definitions and Measurement Methods,* pp. 49–63. Nat. Bur. Standards Spec. Publ. 503.

Smith, P. P. K. (1977) An electron microscopic study of amphibole lamellae in augite. *Contrib. Mineral. Petrol., 59,* 317–322.

Swed, F. S. and C. Eisenhart (1943) Tables for testing randomness of grouping in a sequence of alternatives. *Ann. Math. Stat., 14,* 66–87.

Tateyama, H., S. Shimoda and T. Sudo (1978) Synthesis and crystal structure of a triple chain silicate, $Na_2Mg_4Si_6O_{16}(OH)_2$. *Contrib. Mineral. Petrol., 66,* 149–156.

Thompson, J. B., Jr. (1970) Geometrical possibilities for amphibole structures: model biopyriboles. *Am. Mineral., 55,* 292–293.

——— (1978) Biopyriboles and polysomatic series. *Am. Mineral., 63,* 239–249.

Trigunayat, G. C. and A. R. Verma (1976) Polytypism and stacking faults in crystals with layer structure. *Phys. Chem. Mater. Layered Struct., 2,* 269–340.

Van Landuyt, J. and S. Amelinckx (1975) Multiple beam direct lattice imaging of new mixed-layer compounds of the bastnaesite–synchisite series. *Am. Mineral., 60,* 351–358.

Veblen, D. R. and C. W. Burnham (1975) Triple-chain biopyriboles: newly discovered intermediate products of the retrograde anthophyllite–talc transformation, Chester, Vermont (abstr.). *Trans. Am. Geophys. Union (EOS), 56,* 1076.

——— and ——— (1976) Biopyriboles from Chester, Vermont: the first mixed-chain silicates. *Geol. Soc. Am. Abstracts with Programs, 8,* 1153.

——— and ——— (1978a) New biopyriboles from Chester, Vermont: I. Descriptive mineralogy. *Am. Mineral., 63,* 1000–1009.

——— and ——— (1978b) New biopyriboles from Chester, Vermont: II. The crystal structures of jimthompsonite, clinojimthompsonite, and chesterite, and the amphibole–mica reaction. *Am. Mineral., 63,* 1053–1073.

——— and P. R. Buseck (1977) Petrologic implications of hydrous biopyriboles intergrown with igneous pyroxene (abstr.). *Trans. Am. Geophys. Union (EOS), 58,* 1242.

———, ——— and C. W. Burnham (1977) Asbestiform chain silicates: new minerals and structural groups. *Science, 198,* 359–365, and cover photograph.

Verma, A. R. and P. Krishna (1966) *Polymorphism and Polytypism in Crystals.* Wiley, New York.

Yamaguchi, Y., J. Akai and K. Tomita (1978) Clinoamphibole lamellae in diopside of garnet lherzolite from Alpe Arami, Bellinzona, Switzerland. *Contrib. Mineral. Petrol., 66,* 263–270.

Manuscript received, December 18, 1978.
accepted for publication, March 29, 1979.